ELSEVIER

Journal of Power Sources 112 (2002) 76–84

JOURNAL OF POWER SOURCES

www.elsevier.com/locate/jpowsour

Studies on electrochemical properties of thionyl chloride reduction by Schiff base metal(II) complexes

Woo-Seong Kim[a], Woo-Jong Sim[b], Kwang-il Chung[b], Yung-Eun Sung[a], Yong-Kook Choi[b,*]

[a]*Department of Materials Science and Engineering, Kwangju Institute of Science and Technology (K-JIST), 1 Oryong-dong, Puk-gu, Kwangju 500-712, South Korea*

[b]*Department of Chemistry & IBS, Chonnam National University, Kwangju 500-757, South Korea*

Received 10 April 2002; accepted 10 June 2002

Abstract

Electrocatalytic effects associated with the reduction of thionyl chloride in a $LiAlCl_4$–$SOCl_2$ electrolyte solution containing Schiff base metal(II) (metal (M): Co, Ni, Cu and Mn) complexes are evaluated by determining the kinetic parameters for the reactions using cyclic voltammetry at a glassy carbon electrode. The charge-transfer process during the reduction of thionyl chloride is affected by the concentration of the catalyst. Catalytic effects are demonstrated from both a shift in the reduction potential for the thionyl chloride in a more positive direction and an increase in peak currents. The reduction of thionyl chloride is diffusion controlled. Catalytic effects are larger for thionyl chloride solutions containing M(II)(1,5-bis(salicylidene imino) pentane) (M(II)(SALPE)) rather than M(II)(1,3-bis(salicylidene imino) propane) (M(II)(SALPR)). Significant improvements in cell performance are found in terms of the both thermodynamics and kinetic parameters for the thionyl chloride reduction. An exchange rate constant, k^0, of 1.89×10^{-8} cm s^{-1} is found at the bare electrode, while larger values of 2.79×10^{-8} to 2.09×10^{-6} cm s^{-1} are observed in the case of the catalyst-supported glassy carbon electrode.

Keywords: Thionyl chloride; Electrocatalytic effect; Schiff base; Primary battery

1. Introduction

The lithium oxyhalide system is known to be one of the best primary batteries. It has the combined characteristics of high-rate capability, high-specific energy, long shelf-life, and low-temperature operation. The electrochemical performance of lithium–thionyl chloride primary batteries has been of significant practical interest over the past several years, and the mechanism of the reduction of thionyl chloride has been studied [1–14]. The system consists of a Li anode, a porous carbon cathode, and a $LiAlCl_4$–$SOCl_2$ electrolyte solution (LITHCO), where $SOCl_2$ acts as both a solvent and a cathode-active material. The Li anode is prevented from reacting with $SOCl_2$ via the formation of a LiCl passivation film [3] on the Li as soon as it is in contact with the $LiAlCl_4$–$SOCl_2$ electrolyte according to the reaction (1):

$$4Li + 2SOCl_2 \rightarrow S + SO_2 + 4LiCl \quad (1)$$

The electrode kinetics of the cathode discharge reaction are rather poor due to the formation of passive LiCl films at the cathode as a result of the above reaction. The film also causes a voltage delay due to its overly passive nature. Many investigators have made attempts to avoid this high passivity problem. One possible approach to the enhancement in cell performance is the addition of catalyst molecules, which accelerate the rate of electron transfer.

Doddapaneni [13,14], after comparing several metal compounds as possible catalysts, found cobalt and iron phthalocyanines to be the most effective. It was also shown that the addition a small amount of metal phthalocyanines improves cell performance by changing both the thermodynamic and kinetic parameters for the reduction of thionyl chloride. Choi and co-workers [11,12] reported on the passivation and catalytic activity of a thionyl chloride solution containing cobalt phenylporphyrins. In this paper, the catalytic effects relative to thionyl chloride reduction were examined by evaluating the electrokinetic parameters of the reaction in a $LiAlCl_4$–$SOCl_2$ solution which contained quadridentate Schiff base metal(II) (metal (M): Co, Ni, Cu and Mn) compounds as catalysts.

* Corresponding author. Tel. +82-62-530-3375; fax: +82-62-530-3389.
E-mail address: ykchoi@chonnam.chonnam.ac.kr (Y.-K. Choi).

0378-7753/02/$ – see front matter
PII: S0378-7753(02)00342-7

2. Experimental

1,3-Diaminopropane, 1,4-diaminobutane, 1,5-diaminopentane, salicylaldehyde, Co(II) acetate tetrahydrate, Ni(II) acetate tetrahydrate, Cu(II) acetate monohydrate, Mn(II) acetate tetrahydrate, sodium hydroxide, methanol and ethanol were used as received from Aldrich. The elemental analysis (carbon, hydrogen, nitrogen) was performed by means of a Foss Heraeus CHN Rapid instrument (Analysentechnik GmbH), and the metal content was determined using a Perkin-Elmer Model 603 atomic absorption spectrometer. Infrared and UV-Vis spectra were recorded with Shimadzu IR-430 infrared and Hitachi-557 UV-Vis spectrophotometers. Thermogravimetric analysis (TGA) was carried out using a Perkin-Elmer Model 2 thermogravimetric analyzer. The molar conductance was measured in DMF at 25 °C by means of a DKK model AO-6 digital conductor meter.

2.1. Preparation of 1,3-bis(salicylidene imino) propane (SALPR)

The quadridentate Schiff base ligands were synthesized using methodology described in our previous reports [15,16]. A 0.1 M solution of 1,3-diaminopropane in ethanol (50 ml) was slowly added to 0.2 M of salicylaldehyde in ethanol (50 ml) under a nitrogen atmosphere. A yellow solid precipitate of 1,3-bis(salicylidene imino) propane (SALPR) was obtained. The precipitate was recrystallized from ethanol and dried under reduced pressure at room temperature: 96% yield; mp 54–55 °C; analysis calculated for $C_{17}H_{18}N_2O_2$: C, 72.32, H, 6.43, N, 9.92; found: C, 71.72, H, 6.39, N, 9.54; UV-Vis/(DMF, λ_{max}, $\varepsilon \times 10^{-4}$ cm^{-1} M^{-1}): 272/(1.93), 306/(2.47), 346/(2.24); IR/(KBr pellet, cm^{-1}): 1636/(C=N), 1612, 1447/(C=C).

2.2. Preparation of 1,4-bis(salicylidene imino) butane (SALBU)

A 0.1 M solution of 1,4-diaminobutane in ethanol (50 ml) was slowly added to 0.2 M of salicylaldehyde in ethanol (50 ml) under a nitrogen atmosphere. This gave a yellow solid precipitate of 1,4-bis(salicylidene imino) butane (SALBU). The precipitate was recrystallized from ethanol and dried under reduced pressure at room temperature: 96% yield; mp 93–95 °C; analysis calculated for $C_{18}H_{20}N_2O_2$: C, 72.95, H, 6.80, N, 9.45; found: C, 73.24, H, 6.80, N, 9.20; UV-Vis/(DMF, λ_{max} $\varepsilon \times 10^{-4}$ cm^{-1} M^{-1}): 272/(2.08), 308/(2.68), 346/(2.44); IR/(KBr pellet, cm^{-1}): 1632/(C=N), 1609, 1497/(C=C).

2.3. Preparation of 1,5-bis(salicylidene imino) pentane (SALPE)

A 0.1 M solution of 1,5-diaminopentane in ethanol (50 ml) was slowly added to 0.2 M of salicylaldehyde in ethanol (50 ml) under a nitrogen atmosphere gave a yellow solid precipitate of 1,5-bis(salicylidene imino) pentane (SALPE). The precipitate was recrystallized from ethanol and dried under reduced pressure at room temperature: 95% yield; mp 64–65 °C; analysis calculated for $C_{19}H_{22}N_2O_2$: C, 73.52, H, 7.14, N, 9.02; found: C, 7354, H, 7.16, N, 8.93; UV-Vis/(DMF, λ_{max}, $\varepsilon \times 10^{-4}$ m^{-1} M^{-1}): 274/(2.13), 308/(2.42), 348/(2.56); IR/(KBr pellet, cm^{-1}): 1634/(C=N), 1609, 1497/(C=C).

2.4. Preparation of complexes

The M(II)(SALPR), M(II)(SALBU) and M(II)(SALPE) complexes (M: Co, Ni, Cu and Mn) were prepared by the addition of 0.01 M of ligands which were mixed with 0.02 M sodium hydroxide in hot ethanol (100 ml) to the same volume of 0.01 M M(II) acetate, respectively, in water (30 ml) under a nitrogen atmosphere with stirring. The M(II) complexes were obtained as precipitates. These complexes were recrystallized from ethanol and dried under reduced pressure.

[Co(II)(SALPR)$(H_2O)_2$]: 95% yield; mp 306 ± 2 °C; analysis calculated $C_{17}H_{22}N_2O_4Co$: C, 54.41, H, 5.37, N, 7.46, Co, 15.70; found: C, 53.98, H, 5.25, N, 7.31, Co, 15.81; UV-Vis/(DMF, λ_{max}, $\varepsilon \times 10^{-4}$ cm^{-1} M^{-1}): 272/(2.64), 396/(0.84); IR/(KBr pellet, cm^{-1}): 1628/(C=N), 1539, 1468/(C=C), 758/(Co–N), 582/(Co–O); TGA/(weight loss, %): 9.71 at ∼207 °C, 32.86 at 207–416 °C, 32.11 at 416–652 °C, 25.32 at ∼652 °C.

[Co(II)(SALBU)$(H_2O)_2$]: 93% yield; mp 342 ± 2 °C; analysis calculated for $C_{18}H_{24}N_2O_4Co$: C, 55.53, H, 5.70, N, 7.20, Co, 15.14; found: C, 54.14, H, 5.59, N, 7.17, Co, 15.02; UV-Vis/(DMF, λ_{max}, $\varepsilon \times 10^{-4}$ cm^{-1} M^{-1}): 274/(2.42), 366/(2.02); IR/(KBr pellet, cm^{-1}): 1618/(C=N), 1547, 1472/(C=C), 760/(Co–N), 586/(Co–O); TGA/(weight loss, %): 9.41 at ∼193 °C, 30.07 at 193–384 °C, 35.79 at 384–686 °C, 24.73 at 686 °C.

[Co(II)(SALPE)$(H_2O)_2$]: 95% yield; mp 205 ± 2 °C; analysis calculated for $C_{19}H_{26}N_2O_4Co$: C, 56.58, H, 6.00, N, 6.95, Co, 14.61; found: C, 55.43, H, 5.88, N, 7.04, Co, 14.70; UV-Vis/(DMF, λ_{max}, $\varepsilon \times 10^{-4}$ cm^{-1} M^{-1}): 274/(2.04), 366/(0.86); IR/(KBr pellet, cm^{-1}): 1609/(C=N), 1535, 1445/(C=C), 756/(Co–N), 586/(Co–O); TGA/(weight loss, %): 9.38 at ∼219 °C, 33.43 at 219–399 °C, 34.18 at 399–640 °C, 23.01 at ∼640 °C.

[Ni(II)(SALPR)$(H_2O)_2$]: 95% yield; mp 285 ± 2 °C; analysis calculated for $C_{17}H_{22}N_2O_4Ni$: C, 54.41, H, 5.60, N, 7.56, Ni, 15.71; found: C, 54.02, H, 5.57, N, 7.53, Ni, 15.64; UV-Vis/(DMF, λ_{max}, $\varepsilon \times 10^{-4}$ cm^{-1} M^{-1}): 276/(1.41), 389/(1.35); IR/(KBr pellet, cm^{-1}): 1622/(C=N), 1541, 1475/(C=C), 752/(Ni–N), 464/(Ni–O); TGA/(weight loss, %): 9.70 at ∼262 °C, 33.95 at 262–628 °C, 31.87 at 628–678 °C, 24.88 at 678 °C.

[Ni(II)(SALBU)$(H_2O)_2$]: 88% yield; mp 356 ± 2 °C; analysis calculated for $C_{18}H_{24}N_2O_4Ni$: C, 54.44, H, 5.37, N, 7.47, Ni, 15.65; found: C, 55.73, H, 5.06, N, 7.72, Ni, 15.59;

UV-Vis/(DMF, λ_{max}, $\varepsilon \times 10^{-4}$ cm^{-1} M^{-1}): 276/(2.36), 369/(1.69); IR/(KBr pellet, cm^{-1}): 1616/(C=N), 1541, 1470/(C=C), 750/(Ni–N), 463/(Ni–O); TGA/(weight loss, %): 9.33 at ~235 °C, 29.56 at 235–437 °C, 37.60 at 437–642 °C, 23.51 at ~642 °C.

[Ni(II)(SALPE)$(H_2O)_2$]: 90% yield; mp 205 ± 2 °C; analysis calculated for $C_{19}H_{26}N_2O_4Ni$: C, 55.57, H, 5.70, N, 7.20, Ni, 15.09; found: C, 55.11, H, 5.35, N, 7.73, Ni, 15.28; UV-Vis/(DMF, λ_{max}, $\varepsilon \times 10^{-4}$ cm^{-1} M^{-1}): 287/(2.51), 327/(1.88); IR/(KBr pellet, cm^{-1}): 1614/(C=N), 1541, 1472/(C=C), 754/(Ni–N), 463/(Ni–O); TGA/(weight loss, %): 9.05 at ~249 °C, 42.67 at 249–370 °C, 25.32 at 370–651 °C, 22.96 at ~651 °C.

[Cu(II)(SALPR)]: 88% yield; mp 324 ± 2 °C; analysis calculated for $C_{17}H_{18}N_2O_2Cu$: C, 59.38, H, 4.69, N, 8.09, Cu, 18.48; found: C, 59.15, H, 4.67, N, 8.09, Cu, 18.93; UV-Vis/(DMF, λ_{max}, $\varepsilon \times 10^{-4}$ cm^{-1} M^{-1}): 270/(1.74), 369/(0.71); IR/(KBr pellet, cm^{-1}): 1616/(C=N), 1539, 1470/(C=C), 760/(Cu–N), 584/(Cu–O); TGA/(weight loss, %): 1.08 at ~213 °C, 39.64 at 213–638 °C, 31.27 at 638–692 °C, 28.01 at ~692 °C.

[Cu(II)(SALBU)]: 87% yield; mp 313 ± 2 °C; analysis calculated for $C_{18}H_{20}N_2O_2Cu$: C, 60.41, H, 5.07, N, 7.83, Cu, 17.76; found: C, 60.17, H, 5.05, N, 7.71, Cu, 1667; UV-Vis/(DMF, λ_{max}, $\varepsilon \times 10^{-4}$ cm^{-1} M^{-1}): 274/(2.23), 378/(1.02); IR/(KBr pellet, cm^{-1}): 1609/(C=N), 1533, 1468/(C=C), 762/(Cu–N), 586/(Cu–O); TGA/(weight loss, %): 0.86 at ~184 °C, 39.18 at 184–576 °C, 32.33 at 576–627 °C, 27.63 at ~627 °C.

[Cu(II)(SALPE)]: 85% yield; mp 258 ± 2 °C; analysis calculated for $C_{19}H_{22}N_2O_2Cu$: C, 61.36, H, 5.42, N, 7.53, Cu, 17.08; found: C, 60.36, H, 5.21, N, 7.75, Cu, 17.18; UV-Vis/(DMF, λ_{max}, $\varepsilon \times 10^{-4}$ cm^{-1} M^{-1}): 274/(2.26), 367/(1.13); IR/(KBr pellet, cm^{-1}): 1622/(C=N), 1601, 1462/(C=C), 762/(Cu–N), 586/(Cu–O); TGA/(weight loss, %): 0.94 at ~216 °C, 40.22 at 216–542 °C, 32.96 at 542–646 °C, 25.88 at ~646 °C.

[Mn(II)(SALPR)$(H_2O)_2$]: 90% yield; mp 324 ± 2 °C; analysis calculated for $C_{17}H_{22}N_2O_4Mn$: C, 54.13, H, 5.47, N, 7.51, Mn, 14.96; found: C, 53.98, H, 5.32, N, 7.27, Mn, 14.86; UV-Vis/(DMF, λ_{max}, $\varepsilon \times 10^{-4}$ cm^{-1} M^{-1}): 274/(2.54), 368/(1.66); IR/(KBr pellet, cm^{-1}): 1622/(C=N), 1540, 1472/(C=C), 773/(Mn–N), 598/(Mn–O); TGA/(weight loss, %): 9.69 at ~264 °C, 33.43 at 264–618 °C, 31.22 at 618–686 °C, 23.88 at 686 °C.

[Mn(II)(SALBU)$(H_2O)_2$]: 88% yield; mp 256 ± 2 °C; analysis calculated $C_{18}H_{24}N_2O_4Mn$: C, 55.73, H, 5.71, N, 7.22, Mn, 14.39; found: C, 53.98, H, 5.65, N, 733, Mn, 14.22; UV-Vis/(DMF, λ_{max}, $\varepsilon \times 10^{-4}$ cm^{-1} M^{-1}): 276/(2.52), 366/(1.56); IR/(KBr pellet, cm^{-1}): 1618/(C=N), 1540, 1472/(C=C), 760/(Mn–N), 598/(Mn–O); TGA/(weight loss, %): 9.33 at ~224 °C, 30.22 at 224–406 °C, 36.82 at 406–667 °C, 23.21 at ~667 °C.

[Mn(II)(SALPE)$(H_2O)_2$]: 86% yield; mp 247 ± 2 °C, analysis calculated for $C_{19}H_{26}N_2O_4Mn$: C, 56.86, 6.03, N, 6.98, Mn, 13.91; found: C, 54.33, H, 5.89, N, 7.01, Co, 13.66; UV-Vis/(DMF, λ_{max}, $\varepsilon \times 10^{-4}$ cm^{-1} M^{-1}) 276/(2.52), 366/(1.44); IR/(KBr pellet, cm^{-1}): 1608/(C=N), 1540, 1470/(C=C), 756/(Mn–N), 591/(Mn–O); TGA/(weight loss, %): 9.29 at ~234 °C, 30.43 at 234–406 °C, 37.88 at 406–655 °C, 21.99 at 655 °C.

2.5. Electrochemistry

The electrochemical reduction of thionyl chloride was carried out by means of cyclic voltammetry. A jacketed, single compartment cell housed a glassy carbon working (geometric area, 0.071 cm^2), a platinum wire counter electrode, and a lithium wire reference electrode. The glassy carbon electrode was polished to a mirror finish with 1 μm alumina powder, then cleaned in an ultrasonic bath to remove solid particles, and finally rinsed several times with double-distilled, deionized water before use. A 1.53 M $LiAlCl_4$–$SOCl_2$ electrolyte solution was used. All experiments were conducted in a glove box under an atmosphere of argon. A Princeton Applied Research (PAR) 273 potentiostat/galvanostat interfaced with a microcomputer through an IEEE-488 bus was used for electrochemical measurements.

3. Results and discussion

Quadridentate Schiff base M(II) complexes were prepared and characterized by UV-Vis, IR, TGA, and elemental analysis. The results of elemental analyses of the Schiff base ligands and their complexes are in good agreement with the expected composition of the proposed complexes (Fig. 1). All complexes are insoluble in water but soluble in both aprotic solvents and $SOCl_2$. The positive charges of

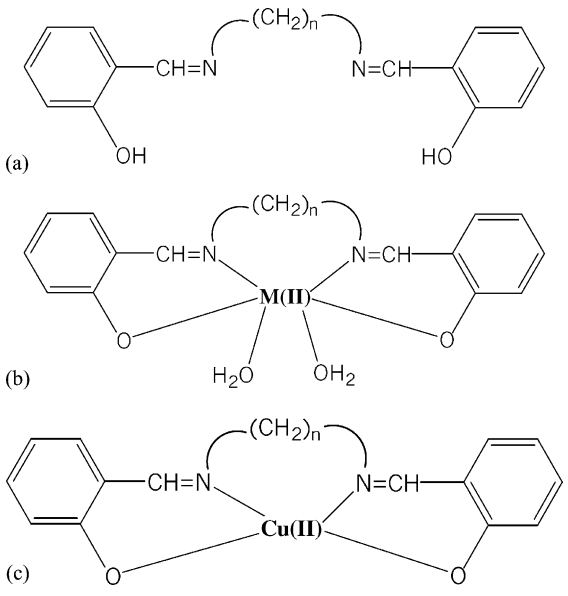

Fig. 1. Structures of ligands and complexes: (a) ligands ($n = 3$; $SALPRH_2$, $n = 4$; $SALBUH_2$, $n = 5$; $SALPEH_2$); (b) M(II) complexes (M: Co, Ni, Mn); and (c) Cu(II) complex.

M(II) are possibly neutralized by the two phenoxy groups. The IR spectra of Co(II), Ni(II), Mn(II) complexes show broad ν(OH) bands which correspond to the free ligands at 3400 cm^{-1}, but these are not found in the case of the Cu(II) complexes. The origin of the broad ν(OH) bands is bonding to H_2O. All of the IR spectra of M(II) complexes show typical bands for a Schiff base with strong peaks assigned to ν(C=N) in the 1608–1628 cm^{-1} region. It can be seen that the ν(C=N) bands in the complex are shifted to the lower energy regions by 4–28 cm^{-1} in the case of the corresponding free ligands. According to Ueno and Martell [17], characteristic absorption bands for M(II)–N and M(II)–O bonds in complexes appear, respectively, in the spectral regions of 650–850 and 400–600 cm^{-1}. Therefore, the two absorption bands at 750–773 and 463–598 cm^{-1} are assigned as M(II)–N and M(II)–O bonds. UV-Vis spectra of the M(II) complexes obtained in DMSO show π–π^* ligand field absorption band at 270–287 nm and a d–π^* charge-transfer band at 327–396 nm. Co(II), Ni(II), Mn(II) complexes show the TGA curve decreasing in weight at 184–264 °C and with subsequent decomposition. Thermal gravimetric analysis data support the conclusion that the M(II) complexes contain two water molecules.

The catalytic activity for the electrochemical reduction of thionyl chloride by metal phthalocyanines has been investigated by Doddapaneni [14]. Two voltammetric peaks were reported for the reduction of thionyl chloride in the presence of these catalysts and the catalytic activity was attributed to the formation of a thionyl chloride adduct with a phthalocyanine molecule, followed by a two-step fast electron transfer to the adduct. The two consecutive electron-transfer reactions were assumed to be

$$\text{M-Pc} \cdot \text{SOCl}_2 + e^- \rightarrow \text{M-Pc} \cdot \text{SOCl}^\bullet + \text{Cl}^- \quad (2)$$

$$\text{M-Pc} \cdot \text{SOCl}^\bullet + e^- \rightarrow \text{M-Pc} + \tfrac{1}{2}\text{S} + \tfrac{1}{2}\text{SO}_2 + \text{Cl}^- \quad (3)$$

which explain the two voltammetric that were observed peaks.

Bernstein and Lever [18] described the reaction as a typical catalytic EC reaction after extensive experiments using 1,2-dichlorobenzene. Thus, the two cyclic voltammetric peaks observed during the catalytic reduction correspond to Co(III)-Pc to, first, Co(II)-Pc and then to Co(I)-Pc. The overall catalytic cycle is

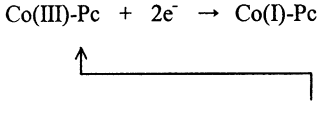

(4)

These investigators provided convincing evidence that $SOCl_2$ oxidizes Co(I)-Pc through a two-electron-transfer reaction. Bernstein and Lever's conclusions on the thermodynamic and kinetic requirements for the electrocatalysts show that: (i) the thermodynamic reduction potential of $SOCl_2$ must be more positive than the oxidation potentials of the metal phthalocyanines; (ii) the electron-transfer kinetics must be more favorable at a given electrode for these compounds than for thionyl chloride. While the thermodynamic requirement is dependent on the electron affinity of the central metal ion of a catalyst molecule, the latter would be easily satisfied given that most metal phthalocyanines are known to undergo reversible reactions due to their favorable molecular size as well as their molecular geometry.

The catalytic effects of M(II)(SALPR), M(II)(SALBU) and M(II)(SALPE) complexes on the reduction of thionyl chloride at a glassy carbon electrode were evaluated by determination of the kinetic parameters using cyclic voltammetry. Peak currents and peak potentials obtained from the cyclic voltammograms are plotted in Fig. 2 as a function of the catalyst concentration for the Co(II)(SALPE) complex. The magnitude of the reduction current appears to be dependent on the concentration of catalyst in the thionyl chloride solution. This effect is observed for all complexes, although to different extents. An optimum concentration exists for each catalyst at around 0.8 mM because the rate-limiting step for reduction of the thionyl chloride is dependent on the electron transfer at the electrode surface.

Cyclic voltamograms for thionyl chloride reduction in the presence of optimum concentrations of M(II) complexes at a glassy carbon electrode are presented in Fig. 3. The sharp current drop at the less positive side appears to be due to passivation of the electrode by lithium chloride [7]. The catalytic effects are clearly demonstrated by the shift in the reduction potential for thionyl chloride towards a positive direction, which result in a decrease in the overpotential. This indicates that the Schiff base complexes used in this study act as catalysts for the reduction of thionyl chloride. In particular, the peak potential is shifted by about 110 mV in the positive direction and the peak current is increased by about 186% in Co(II)(SALPE). Therefore, it is concluded that the compounds show good catalytic activities at a glassy carbon electrode. These results are in agreement with those reported by Doddapaneni [13] for the reduction of a $SOCl_2$ solution of metal phthalocyanine.

An extensive number of cyclic voltammetric experiments were conducted only at the 'optimum' catalyst concentration to evaluate the kinetic parameters for the reactions. The peak currents and potentials observed for the reduction of thionyl chloride are summarized in Table 1. In general, the peak potential and peak current are increased for longer chain catalysts. The reason for this is the steric hindrance of the transition metal, which reacts with the thionyl chloride. A series of cyclic voltammograms recorded at various scan rates in thionyl chloride solutions of Co(II) complexes are presented in Fig. 4. The current decays faster than in the Cottrellian fashion beyond the cyclic voltammogram peak potential. As discussed above, this phenomenon appears to be due to some level of passivation of the electrode surface during the reduction of thionyl chloride. To establish, whether the electron transfer is a diffusion controlled or a

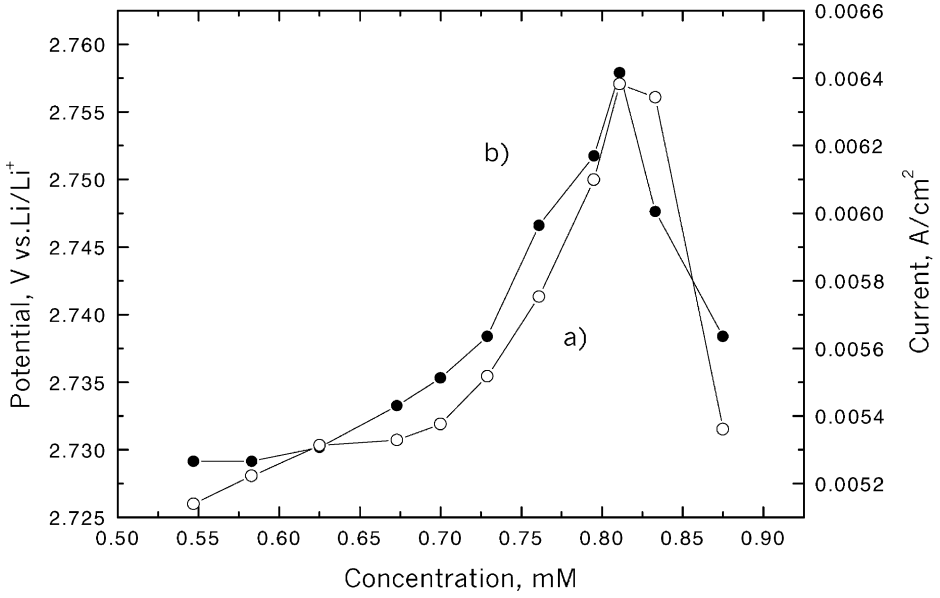

Fig. 2. Plots of peak currents and peak potentials vs. concentration of catalyst for reduction of $SOCl_2$ solution containing [Co(II)(SALPE)$(H_2O)_2$]: (a) peak current; and (b) peak potential. Scan rate: 50 mV s^{-1}.

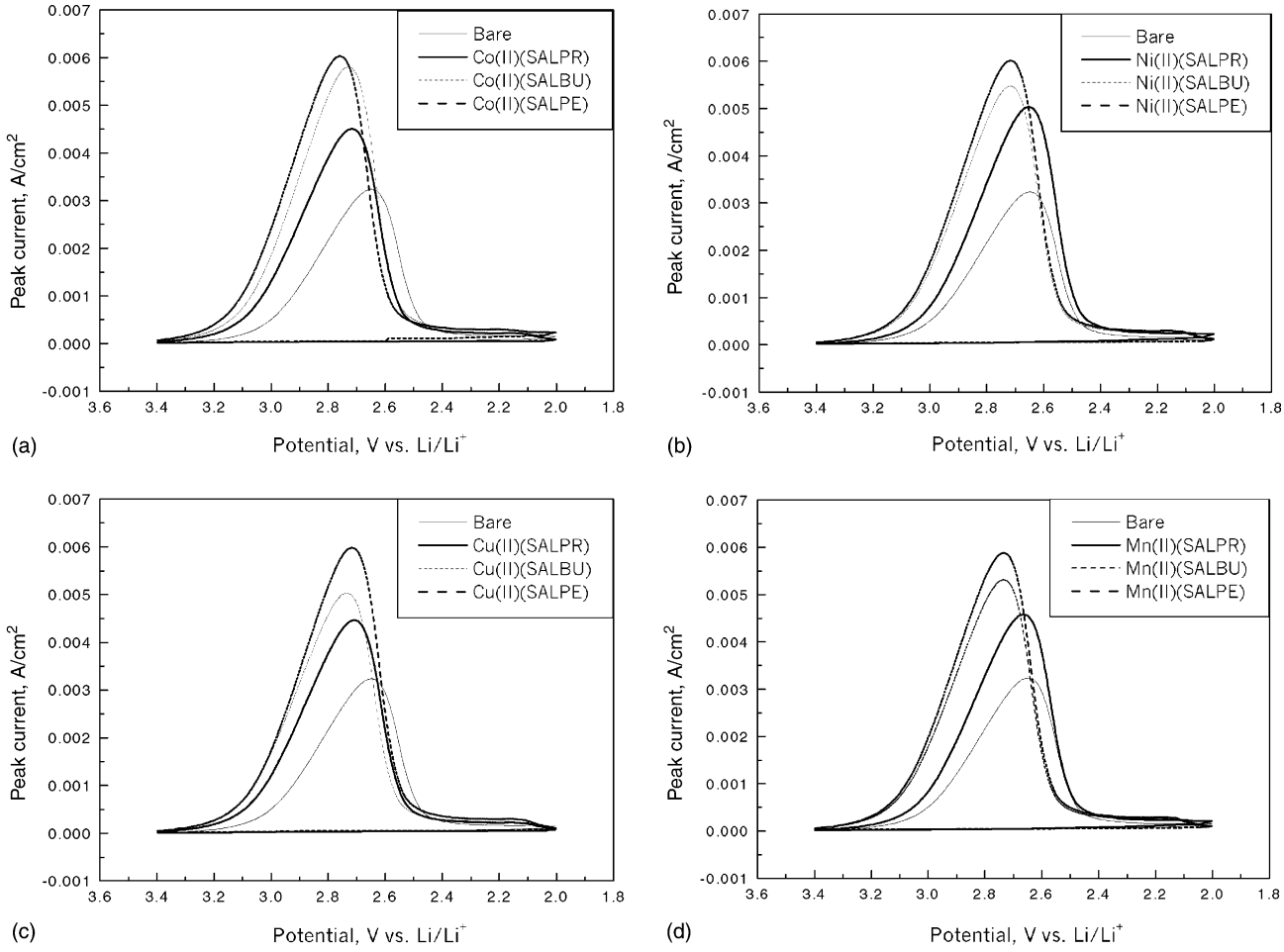

Fig. 3. Cyclic voltammograms for reduction of $SOCl_2$ solution at optimum concentrations containing: (a) Co(II); (b) Ni(II); (c) Cu(II); and (d) Mn(II) complexes. Scan rate: 50 mV s^{-1}.

Table 1
Peak potentials and peak currents for $SOCl_2$ reduction at glassy carbon electrode (scan rate: 50 mV s^{-1})

Catalysts	Concentration (mM)	Peak potential E_p (V)	Peak current i_p (A)
Bare	–	2.649	0.000243
Co(II)(SALPR)$(H_2O)_2$	0.81	2.682	0.000338
Co(II))(SALBU)$(H_2O)_2$	0.79	2.716	0.000449
Co(II))(SALPE)$(H_2O)_2$	0.81	2.759	0.000453
Ni(II))(SALPR)$(H_2O)_2$	0.80	2.656	0.000378
Ni(II))(SALBU)$(H_2O)_2$	0.79	2.712	0.000411
Ni(II))(SALPE)$(H_2O)_2$	0.79	2.713	0.000452
Cu(II))(SALPR)	0.79	2.709	0.000358
Cu(II)(SALBU)	0.79	2.715	0.000378
Cu(II)(SALPE)	0.80	2.716	0.000449
Mn(II))(SALPR)$(H_2O)_2$	0.79	2.664	0.000344
Mn(II))(SALBU)$(H_2O)_2$	0.81	2.734	0.000399
Mn(II))(SALPE)$(H_2O)_2$	0.79	2.735	0.000442

surface process, cyclic voltammetric peak currents are plotted against the square root of the scan rate ($v^{1/2}$). The results obtained at the glassy carbon electrode under 'optimum' conditions are given in Fig. 5. The data indicate that thionyl chloride reduction at the glassy carbon electrode is controlled by diffusion of the electroactive compound. The peak current from cyclic voltammetry for an irreversible case is given as follows [19]:

$$i_p = (2.99 \times 10^5) n(\alpha n_a)^{1/2} A C_0^* D_0^{1/2} v^{1/2} \quad (5)$$

where n is the number of electrons transferred, α the transfer coefficient, n_a the apparent number of electrons transferred, A the electrode area in cm^2, C_0^* the bulk concentration of an electroactive compound in mol cm^{-3}, D_0 is the diffusion coefficient of the electroactive compound or other charge carrier in $cm^2\ s^{-1}$. A plot of i_p versus $v^{1/2}$ will permit the diffusion coefficient of thionyl chloride with known αn_a to be obtained. From the relationship of i_p with E_p [19]:

$$i_p = 0.227 nFAC_0^* k^0 \exp\left[-\left\{\frac{\alpha n_a F}{RT}\right\}(E_p - (E^0)')\right] \quad (6)$$

where k^0 is the exchange rate constant (cm s^{-1}), $(E^0)'$ is the standard electrode potential (V). A plot of $\ln(i_p)$ versus $E_p - (E^0)'$ should yield a straight line with a slope, $\alpha n_a F/$

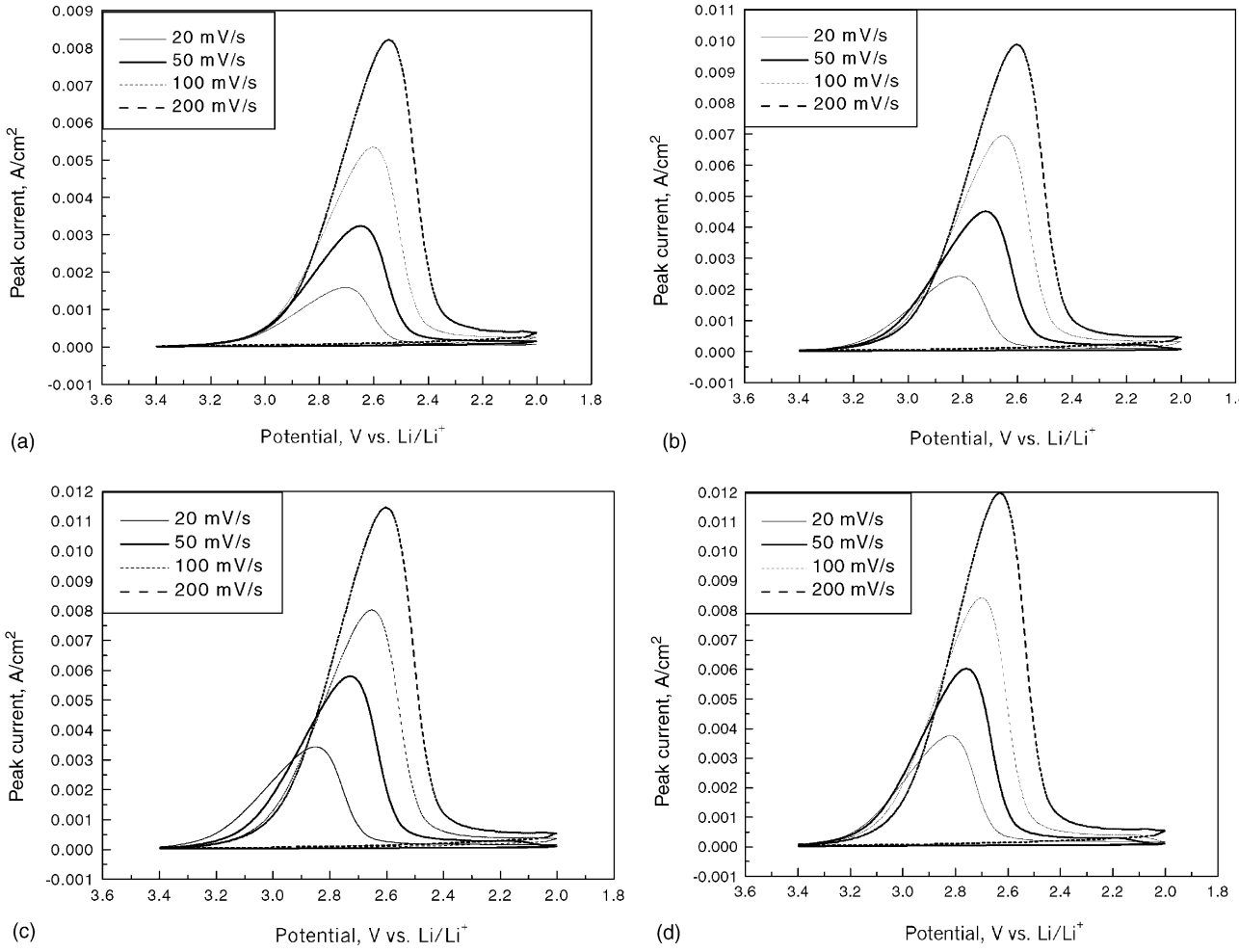

Fig. 4. Scan rate dependency of voltammograms for reduction of $SOCl_2$ solution containing: (a) bare; (b) Co(II)(SALPR)$(H_2O)_2$; (c) Co(II)(SALBU)$(H_2O)_2$; and (d) Co(II)(SALPE)$(H_2O)_2$ complexes. Scan rate: (a) 20; (b) 50; (c) 100; and (d) 200 mV s^{-1}.

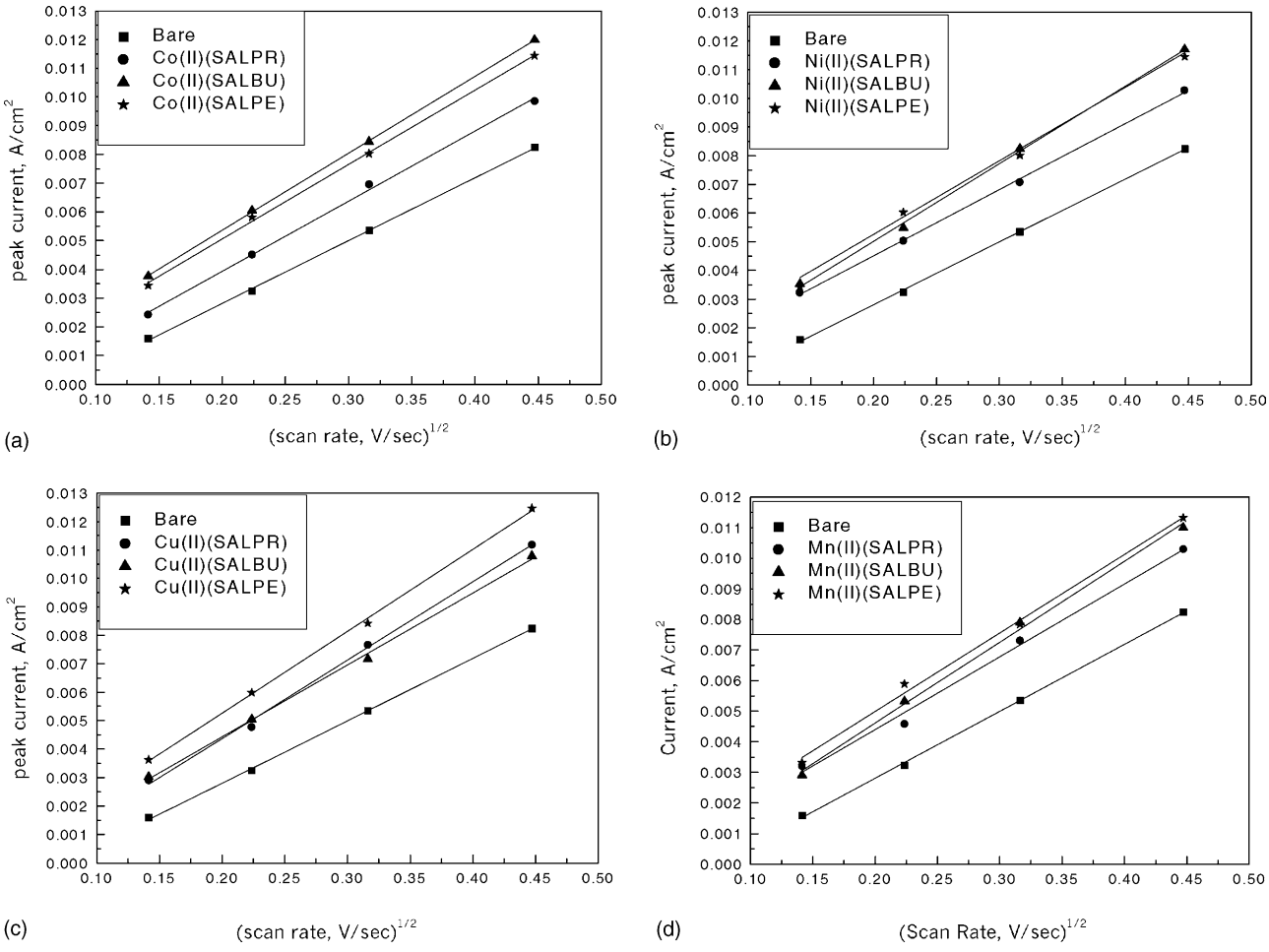

Fig. 5. Plots of peak current vs. $v^{1/2}$ for reduction of $SOCl_2$ at optimum concentrations containing: (a) Co(II); (b) Ni(II); (c) Cu(II); and (d) Mn(II) complexes.

RT, and an intercept, $\ln(0.227nFAC_0^*k^0)$, from which αn_a and k^0 values can be calculated, respectively. In these calculations, the thermodynamic volume for E^0, viz., 3.734 V versus Li/Li^+, is used as obtained from. Eq. (1) using the free energies of formation for the reactants and product [6]. The $\ln(i_p)$ versus $E_p - (E^0)'$ plots are shown in Fig. 6 for the reduction of $SOCl_2$ at the glassy carbon electrode. The αn_a value obtained from this equation can be used to determine $D_0^{1/2}$ in Eq. (5).

Kinetic parameters calculated from these plots at 'optimum' catalyst concentrations are listed in Table 2. The exchange rate constants k^0, was determined to be 1.89×10^{-8} cm s^{-1} at

Table 2
Kinetic parameters for $SOCl_2$ reduction at glassy carbon electrode

Catalysts	Concentration	αn_a	D_0 ($cm^2\ s^{-1}$)	k^0 (cm s^{-1})
Bare	–	0.14	5.67×10^{-9}	1.89×10^{-9}
Co(II)(SALPR)$(H_2O)_2$	0.81	0.14	1.10×10^{-8}	3.75×10^{-7}
Co(II)(SALBU)$(H_2O)_2$	0.79	0.16	1.34×10^{-8}	2.11×10^{-7}
Co(II)(SALPE)$(H_2O)_2$	0.81	0.15	1.24×10^{-8}	3.67×10^{-7}
Ni(II)(SALPR)$(H_2O)_2$	0.80	0.19	8.19×10^{-9}	3.93×10^{-8}
Ni(II)(SALBU)$(H_2O)_2$	0.79	0.13	1.59×10^{-8}	5.45×10^{-7}
Ni(II)(SALPR)$(H_2O)_2$	0.79	0.11	1.81×10^{-8}	2.09×10^{-6}
Cu(II)(SALPR)	0.79	0.18	1.23×10^{-8}	7.46×10^{-8}
Cu(II)(SALBU)	0.79	0.18	1.04×10^{-8}	1.07×10^{-7}
Cu(II)(SALPE)	0.80	0.16	1.50×10^{-8}	2.23×10^{-7}
Mn(II)(SALPR)$(H_2O)_2$	0.79	0.19	8.47×10^{-9}	2.79×10^{-8}
Mn(II)(SALBU)$(H_2O)_2$	0.81	0.14	1.41×10^{-8}	4.20×10^{-7}
Mn(II)(SALPE)$(H_2O)_2$	0.79	0.13	1.44×10^{-8}	7.10×10^{-7}

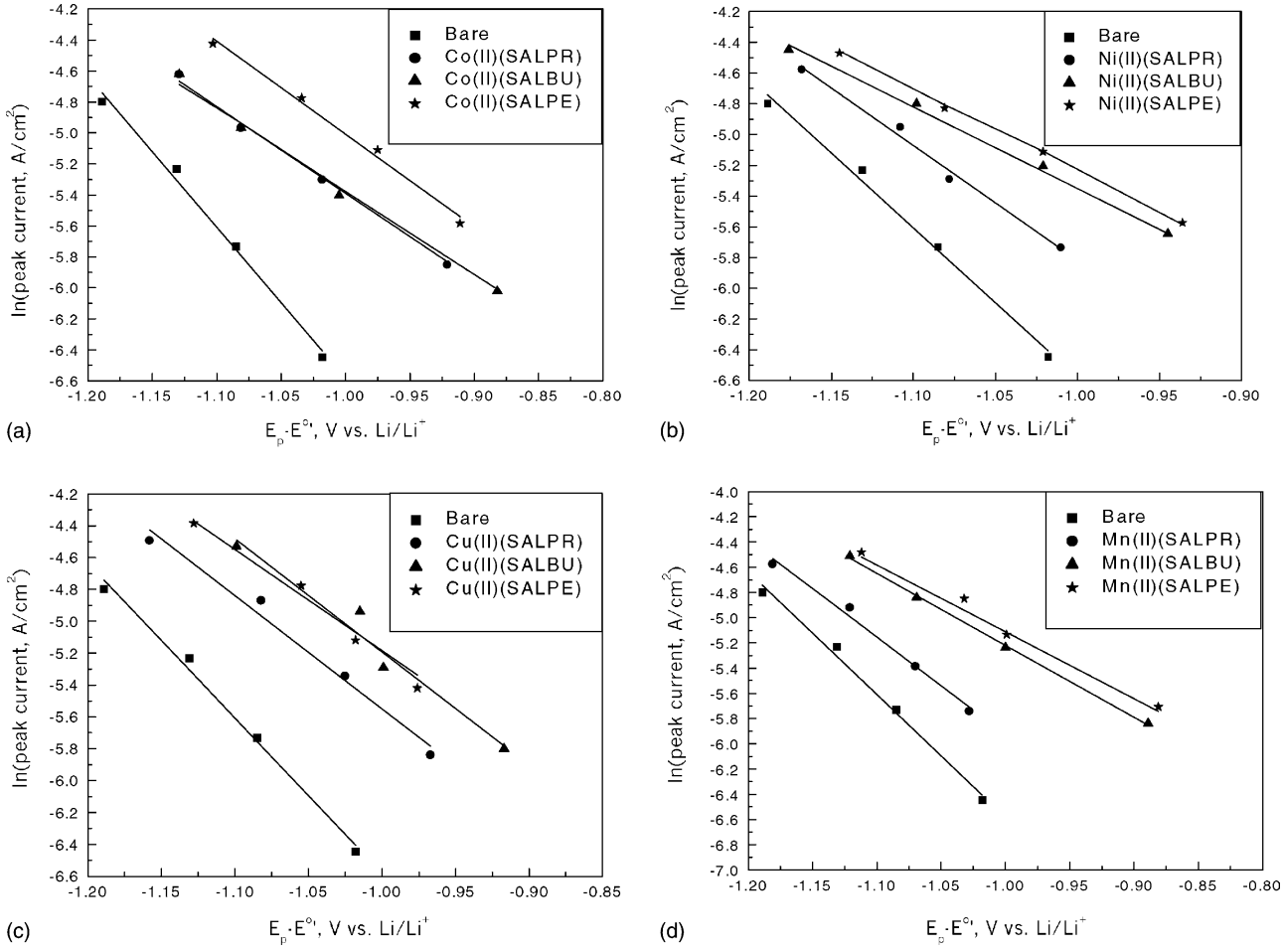

Fig. 6. Plots of $\ln(i_p)$ vs. $(E_p - (E^0)')$ for reduction of $SOCl_2$ at optimum concentration containing: (a) Co(II); (b) Ni(II); (c) Cu(II); and (d) Mn(II) complexes.

the bare glassy carbon electrode at room temperature. On the other hand, the value was 2.79×10^{-8} to 2.09×10^{-6} cm s^{-1} at the catalyst supported glassy carbon electrode. The increase in exchange rate constant indicates a significant improvement in cell performance. Therefore, most of the enhancement can be attributed to the catalytic effects of the Shciff base complexes. As shown in Tables 1 and 2, catalytic effects are slightly larger in thionyl chloride solution containing M(II)(SALPE) than M(II)(SALPR) or M(II)(SALBU) complexes, which is probably due to steric factors.

4. Conclusions

It is clear that some Schiff base transition metal compounds show sizeable catalytic activity for the reduction of thionyl chloride. From the earlier results, it is concluded that

(i) catalyst molecules are reduced on the electrode surface, which in turn reduces thionyl chloride and results in the generation of oxidized catalyst molecules to complete the catalytic cycle;
(ii) an optimum concentration exists for each catalyst;
(iii) relative catalytic effects are slightly larger in thionyl chloride solution containing M(II)(SALPE) complexes compared to M(II)(SALPR) or M(II)(SALBU).

Acknowledgements

This work was supported by the Korean Science and Engineering Foundation through the Region Research Center of HECS of Chonnam National University, 2001. WSK and YES acknowledge financial support from the Ministry of Commerce, Industry and Energy and the BK 21 Project of the Ministry of Education.

References

[1] Y.-K. Choi, W.-S. Kim, K. Chung, M.-W. Chung, H.-P. Nam, Microchem. J. 65 (2000) 3.
[2] W.-S. Kim, M.-S. Shin, Y.-K. Choi, K.-H. Chjo, Bull. Kor. Chem. Soc. 14 (1993) 313.

[3] D.J. Salmon, M.E. Adamczyk, L.L. Hendricks, L.L. Abels, J.C. Hall, in: H.V. Venkatasetty (Ed.), Proceedings of the Electrochemical Society on Lithium Battery Technology, Pennigton, NJ, USA, 1981.
[4] A.J. Hills, N.A. Hampson, J. Power Sources 24 (1988) 253.
[5] O.A. Baturina, L.S. Kanevsky, V.S. Bagotsky, V.V. Volod'ko, A.L. Karasev, A.A. Revina, J. Power Sources 36 (1991) 127.
[6] V.S. Bagotsky, V.E. Kazarinov, Yu.M. Volfkovich, L.S. Kanevsky, L.A. Beketayeva, J. Power Sources 26 (1989) 427.
[7] K.M. Abraham, J. Power Sources 34 (1991) 81.
[8] C.R. Schlaikjer, J. Power Sources 26 (1989) 161.
[9] M.-S. Shin, W.-S. Kim, K.-H. Chjo, Y.-K. Choi, Bull. Kor. Chem. Soc. 16 (1995) 205.
[10] W.-S. Kim, K. Chung, S.-K. Kim, S. Jeon, Y.-H. Kim, Y.-F. Sung, Y.-K. Choi, Bull. Kor. Chem. Soc. 21 (2000) 571.
[11] Y.-K. Choi, B.-S. Kim, S.-M. Park, J. Electrochem. Soc. 140 (1993) 11.
[12] W.-S. Kim, Y.-K. Choi, K.-H. Chjo, Bull. Kor. Chem. Soc. 15 (1994) 456.
[13] N. Doddapaneni, in: Proceedings of the 30th Power Sources Symposium, Electrochemical Society, Atlantic City, NJ, USA, 1982, p. 169.
[14] N. Doddapaneni, in: Proceedings of the Symposium on the Chemistry and Physics of Electrocatalysis, Electrochemical Society, Pennington, NJ, USA, 1994, p. 630.
[15] Y.-K. Choi, K.-H. Chjo, K.-H. Park, Bull. Kor. Chem. Soc. 16 (1995) 21.
[16] Y.-K. Choi, K.-H. Chjo, S.-M. Park, N. Doddapaneri, J. Electrochem. Soc. 142 (1995) 4107.
[17] K. Ueno, A.E. Martell, J. Phys. Chem. 60 (1956) 1270.
[18] P.A. Bernstein, A.B.P. Lever, Inorg. Chem. 29 (1990) 608.
[19] A.J. Bard, L.R. Faulkner, Electrochemical Methods, Wiley, NY, USA, 1980 (Chapter 6).